



Published in final edited form as:

Hepatology. 2017 January ; 65(1): 189–201. doi:10.1002/hep.28890.

## Bile acid excess induces cardiomyopathy and metabolic dysfunctions in the heart

Moreshwar Desai<sup>1,\*</sup>,§, Bhoomika Mathur<sup>2,\*</sup>, Zeena Eblimit<sup>1</sup>, Hernan Vasquez<sup>3</sup>, Heinrich Taegtmeier<sup>3</sup>, Saul Karpen<sup>4</sup>, Daniel J. Penny<sup>5</sup>, David D. Moore<sup>6</sup>, and Sayeepriyadarshini Anakk<sup>2,§</sup>

<sup>1</sup>Section of Pediatric Critical Care, Baylor College of Medicine, Houston, TX

<sup>2</sup>Department of Molecular and Integrative Physiology, University of Illinois at Urbana-Champaign, Urbana, IL

<sup>3</sup>Dept. of Cardiology University of Texas Health Sciences Center, Houston, TX

<sup>4</sup>Pediatric Gastroenterology, Emory School of Medicine, Atlanta, GA

<sup>5</sup>Department of Pediatric Cardiology, Baylor College of Medicine, Houston, TX

<sup>6</sup>Department of Molecular and Cellular Biology, Baylor College of Medicine, Houston, TX

### Abstract

Cardiac dysfunction in patients with liver cirrhosis is strongly associated with increased serum bile acid concentrations. Here we show that excess bile acids decrease fatty acid oxidation in cardiomyocytes and can cause heart dysfunction, a cardiac syndrome that we term *Cholecardia*. *Fxr*; *Shp* double knockout (DKO) mice, a model for bile acid overload, display cardiac hypertrophy, bradycardia, and exercise intolerance. In addition, DKO mice exhibit an impaired cardiac response to catecholamine challenge. Consistent with this decreased cardiac function, we show that elevated serum bile acids reduce cardiac fatty acid oxidation both *in vivo* and *ex vivo*. We find that increased bile acid levels suppress expression of *Pgc1a*, a key regulator of fatty acid metabolism, and that *Pgc1a* overexpression in cardiac cells was able to rescue the bile acid-mediated reduction in fatty acid oxidation genes. Importantly, intestinal bile acid sequestration with cholestyramine was sufficient to reverse the observed heart dysfunction in the DKO mice.

**Conclusions**—Overall, we propose that decreased *Pgc1a* expression contributes to the metabolic dysfunction in *Cholecardia*, and that reducing serum bile acid concentrations will be beneficial against metabolic and pathological changes in the heart.

### Keywords

*Cholecardia*; cardiac hypertrophy and dysfunction; metabolic reprogramming; transcriptional co-activators; fatty acid oxidation

\*Equal contribution

§Co-corresponding authors. Address: Sayeepriyadarshini Anakk (Current Address), Department of Molecular & Integrative Physiology, University of Illinois at Urbana-Champaign, Urbana, IL 61801. Tel: 217 300 7905; Fax: 217 244 5858 anakk@illinois.edu, Moreshwar Desai MD, Section of Pediatric Critical Care, Baylor College of Medicine, One Baylor Plaza, Houston, TX 77030. Tel: 832-826-6230; Fax: 832-825-4893 mdesai@bcm.edu

## INTRODUCTION

Cirrhotic cardiomyopathy is a severe cardiovascular condition characterized by rhythm abnormalities, poor contractility and dysfunction<sup>1</sup>. Patients with this pathology have delayed recovery after surgical procedures, and exhibit increased fatality<sup>2-5</sup>. Cirrhotic cardiomyopathy occurs in more than 50% of patients with end stage liver diseases; however, the heart dysfunctions are reversed upon liver transplant<sup>6</sup>. This data suggests that cirrhotic cardiomyopathy is secondary to the liver dysfunction. Despite its clinical significance, there is no treatment currently available for this heart dysfunction since the mechanism(s) that contribute to its pathogenesis remain poorly understood.

Elevated serum bile acids have long been speculated to cause cirrhotic cardiomyopathy<sup>7,8</sup>. In fact, bile was first observed to mediate cardiotoxicity almost a century ago<sup>9</sup>. Increase in bile acids has been shown to reduce heart rate and contractility<sup>10,11</sup> with recent findings indicating that high bile acid levels are linked to arrhythmias in adults as well as fetuses of mothers with obstetric cholestasis<sup>12,13</sup>. Based on these strong associative findings, we propose the term *Cholecardia* to describe a syndrome in which pathological levels of bile acids induce cardiomyopathy.

In the present study, we explored the mechanisms that contribute to *Cholecardia* by characterizing the direct effects of bile acids on the heart using an *in vivo* mouse model, *ex vivo* heart perfusions as well as *in vitro* primary cardiomyocyte cultures and cardiac cell line. We hypothesized that pathological concentrations of bile acids induce functional, metabolic and molecular alterations in the heart and that reducing serum bile acid pools will reverse *Cholecardia*.

## METHODS

### Animal models

The generation of *Fxr* knockout (*FXRKO*), *Shp* knockout (*SHPKO*) and *Fxr;Shp* double knockout mice (DKO) has been described previously<sup>14</sup>. C57BL/6 wild type (WT) male mice were purchased from Harlan (Indianapolis, IN). Mice were housed on a standard 12-hour-light/dark cycle and were fed normal chow and water *ad libitum*. To reduce circulating bile acid levels, DKO mice were fed 2% Cholestyramine-enriched diet for 5 weeks. All the experiments were carried out on 3–5 months old mice as outlined in the *Guide for the Care and Use of Laboratory Animals*, the National Academy of Sciences (NIH publication 86-23, revised 1985) and approved by the Institutional Animal Care and Use Committee at Baylor College of Medicine as well as University of Illinois at Urbana-Champaign.

### Electrocardiographic and echocardiographic studies

Continuous M-mode electrocardiograms were recorded non-invasively in mice (n=6, age: 4–5 months) using EC Genie system (Mouse Systems Inc, Quincy, MA) as described before<sup>15</sup>. Two-dimensional echocardiography (2DE) was performed in the Mouse Phenotyping Core at Baylor College of Medicine on sedated mice (Vevo 770 Digital RF, VisualSonic Inc., Toronto, CA). To evaluate the acute *in vivo* effect of bile acid overload, WT mice were injected with a single dose of either Taurocholic acid (TCA, 100mg/kg) or Lithocholic acid

(LCA, 100mg/kg/dose) dissolved in corn oil for 4 days or corn oil via i.p. prior to echocardiography.

### **Treadmill exercise performance test**

DKO mice were challenged with acute sub-maximal stress in the form of exercise on a treadmill as previously described<sup>15</sup>. First, WT and DKO mice (n=6 per group) were allowed to acclimatize on a treadmill for 5–10 minutes and were then made to run on it with a 10% incline at a speed of 2 meters/min. Speed was gradually increased by 2 meters/min every 2 minutes to a maximal speed of 15 meters/min. The exercise was terminated when the mouse became sedentary on the active electric grid at the end of the treadmill for more than 15 seconds for at least two occasions.

### **Catecholamine challenge and stress echocardiography**

To evaluate the effects of catecholamine on the hearts, WT and DKO mice (n=6 per group) were anesthetized and injected with a single dose of isoprenaline intra-peritoneally (20 µg/kg) (Sigma-Aldrich, St. Louis, MO). Cardiac parameters were evaluated by echocardiography both pre and post injection.

### **Transverse aortic constriction (TAC)**

To determine the response to chronic pressure overload, both WT and DKO mice were subjected to TAC<sup>16</sup>. Prior to isoflurane-induced anesthesia, each mouse received buprenorphine (0.6mg/kg) sub-cutaneously. An incision was made through the ventral chest skin to mid-thorax and between the right innominate and left carotid artery. An aortic constriction was placed by tying a 6-0 black-braided non-absorbable silk suture against a 3mm length of a 27-gauge needle. The tightness of the 0.3 mm constriction was verified 7 days post the bandage using a carotid doppler ultrasound. Contractile function was evaluated every 2 weeks by echocardiography for a period of 8 weeks.

### **Langendorff perfusion experiments**

The retrograde constant flow Langendorff perfusion method was used as previously described<sup>17,18</sup> to evaluate contractility, glucose and fatty acid (oleate) oxidation rates in isolated beating hearts of DKO and WT mice. Further, the effect of a high dose of taurocholic acid (500 µmol/L) was also evaluated on WT hearts. In brief, the hearts were perfused and physiological parameters such as heart rate (cycle beats) and contractility (cycle amplitude) were measured in real time for over 15 minutes on the isolated hearts. To measure glucose and oleate oxidation rates, the perfusate Krebs-Henseleit Buffer (8 mM glucose, 10 µUnits/ml insulin, 1.2 mM sodium oleate conjugated to 3% w/v BSA tracer amounts of [U-<sup>14</sup>C] glucose (40 µCi/l) and [9,10-<sup>3</sup>H] oleate (60 µCi/l) was used. After 5 minutes of normal workload perfusion under constant flow conditions, the hearts were perfused for an additional 15 minutes and both functional as well as metabolic parameters were measured at 5-minute intervals throughout.

### Analysis of total serum bile acid levels and composition

Total serum bile acids were measured using a colorimetric BQ assay kit (SanDiego, CA) according to the manufacturer's protocol. Pooled serum from either WT or DKO mice (n=5–7 mice) were analyzed for individual bile acid contents using LC-MS method in the Metabolomics Core at Baylor College of Medicine. Waters (Waters, Milford, MA) Acquity UPLC BEH C18 column was used for analysis. All bile acids were detected in the negative mode. L-Zeatine was spiked into each sample as internal standard.

### Immuno-blotting

Proteins were extracted from homogenized hearts using standard procedures<sup>19</sup> and the concentration was measured using the Pierce BCA kit (Thermo Scientific, Rockford, IL). After gel electrophoresis and transfer, the blots were probed for expression of various proteins with specific antibodies as described before<sup>15</sup>. Equal protein loading was confirmed by TBP. The results were analyzed by densitometry using Kodak software and reported as fold change compared to control hearts.

### Quantitative real time PCR (qRT-PCR)

The total RNA was isolated from snap frozen hearts (n=5–6 per group) and cultured HL-1 cells (n=4) using TRIzol (Invitrogen, Grand Island, NY) and was subjected to SYBR® Green™ based quantitative real time reverse transcription polymerase chain reaction (qRT-PCR) using mouse specific primer sets, listed in Supplementary Table 2. Relative RNA expression was calculated by delta- delta C<sub>t</sub> method, transcript levels were normalized to 36B4 or 18S as internal controls.

### Histology

Heart tissues from WT and DKO hearts (n=3 each) were fixed in 10% neutral-buffered formalin for 24 hours and subsequently processed. 5 µm thick heart sections were cut, deparaffinized and stained with hematoxylin and eosin (H&E) as well as Masson's Trichrome using standard histological protocols.

### Quantification of cardiomyocyte size using WGA staining

Heart sections were deparaffinized (n=2–3 for WT and DKO mice), and incubated with 10µg Wheat Germ Agglutinin (WGA)-Alexa Fluor 488 (ThermoFisher Scientific) for two hours at room temperature, followed by two washes of 1× PBS washes. The slides were then incubated with Molecular probe NucBlue for 30 minutes at room temperature, and cover slipped. 8–10 fields per section per mice were quantitated using ImageJ WGA macro (<http://www2.le.ac.uk/colleges/medbiopsych/facilities-and-services/cbs/lite/aif/software-1/imagej-macros#WGA>).

### Neonatal mouse cardiomyocyte culture

Cardiomyocytes were isolated from 2-day-old to 3-day-old neonatal WT mouse pups as described previously<sup>15</sup>. Isolated cardiomyocytes ( $5 \times 10^5$  cells/well) were incubated with vehicle (DMSO) or CDCA (100 µM) in a 6-well plate. After 4 hours, cells were harvested for RNA expression by qRT-PCR analysis. Each experiment was performed in duplicates

and repeated three times (n = 3). For each set of treatments, cardiomyocytes were isolated and pooled from 12 to 15 neonatal hearts.

### ***Pgc1a* overexpression studies**

The cardiac HL-1 cell line was cultured as described previously<sup>20</sup>. The *Pgc1a* expression plasmid was obtained as a gift from Dr. JK Kemper's laboratory at University of Illinois, Urbana-Champaign. Approximately 80% confluent HL-1 cells were transfected with 50 ng of *Pgc1a* gene containing pCDNA3.1 plasmid or empty vector using TransIT 2020 reagent. Following 24 hours of transfection, the cells were treated with 100  $\mu$ M CDCA or DMSO for 4 hours and harvested for RNA studies.

### **Statistical analysis**

The data is presented as Mean  $\pm$  SEM (as specified in the legends). Data between 2 groups (DKO and WT) was compared using unpaired t-test, as well as non-parametric Mann-Whitney. Pre- and post- intervention WT or DKO and DKO+CHR comparisons were performed using one-way ANOVA followed by Bonferroni or Newman Keuls post hoc test. *Pgc1a* overexpression analyses were performed using multiple t-test and two-way ANOVA followed by Bonferroni post hoc test. *Ex vivo* perfusion parameters and *in vitro* bile acid incubation experiments were evaluated using non-parametric Mann-Whitney test. Comparisons between WT and either *FXRKO* or *SHPKO* were analyzed using Student t-test. All statistical analyses were done using the Graph-Pad (Prism, San Diego, CA).  $p < 0.05$  was selected as the level of significance.

## **RESULTS**

We have previously described mice in which two key nuclear receptors responsible for maintaining bile acid homeostasis, *Fxr* and *Shp*, are deleted<sup>14</sup>. These double knockout mice (DKO) demonstrate excessive liver injury and accumulate high levels of circulating bile acids along with increases in ALT and AST liver enzymes, and thus are an excellent model of cholestatic liver disease (Supplementary Fig. 1A–B).

### **DKO mice mimic cirrhotic cardiomyopathy with cardiac hypertrophy and functional defects**

Compared to adult wild type (WT), DKO mice showed increased heart weight to tibial length ratio (Fig. 1A). In addition, WGA staining of the cell membrane revealed an increase in cardiomyocytes size (Fig. 1B). However, H&E as well as Masson's Trichrome staining did not show any signs of fibrosis in the heart (Supplementary Fig. 1C–D). We observed a robust induction of the core cytoskeletal proteins,  $\alpha/\beta$  actin and  $\alpha/\beta$  tubulin (Fig. 1C) that is consistent with the observed myocardial dysfunction in DKO hearts<sup>21</sup>. Upon 2D ECHO evaluation<sup>22</sup>, DKO mice displayed abnormal M-mode with decreased left ventricular internal diameter (LVID) in diastole as well as in systole (Fig. 1D). Despite compensatory increases in LV shortening and ejection fraction, DKO mice showed lower cardiac output than WT mice (Fig. 1E). Furthermore, DKO mice showed prolonged QTc and PR intervals on ECG (Fig. 1E), which is specifically observed in human cirrhotic cardiomyopathy and strongly correlates with the observed mortality in adults and children with cirrhosis<sup>23,24</sup>. DKO hearts also displayed bradycardia, increased myosin heavy chain  $\beta$  isoform ( *$\beta$ -MyH7*)

expression along with robust activation of AKT (*Ser473*-phosphorylation) and JNK (*Thr183/Tyr185* phosphorylation) and apoptotic pathways (Supplementary Fig. 2), consistent with pathological cardiac remodeling<sup>25,26</sup>. DKO mice also showed a significant elevation in serum cardiac troponin-2 levels (Fig. 1F), suggesting myocardial injury<sup>27</sup>. These data clearly indicate that DKO mice suffer from cardiac stress and mirror clinical symptoms of cirrhotic cardiomyopathy.

### **DKO mice display impaired response to exogenous cardiac stressors**

Patients with cirrhotic cardiomyopathy have poor response to exercise-induced stress<sup>28</sup> and catecholamines<sup>6</sup>. As expected, DKO mice had significantly decreased performance in terms of both distance and time on the treadmill exercise test compared to WT mice (Fig. 2A–B). Upon isoprenaline challenge, DKO mice took twice the amount of time to achieve the peak increase in heart rate than the controls (Fig. 2C). Moreover, this peak heart rate was slightly blunted in the DKO mice (Fig. 2D) along with reduced response in the ejection fraction (Fig. 2E). The increase in shortening fraction observed in the DKO mice pre-isoprenaline treatment was attenuated post injection indicating repressed  $\beta$ -adrenergic signaling (Fig. 2F). Finally, we examined the ability of DKO hearts to handle pressure overload by performing Transverse Aortic Constriction (TAC). Though decrease in shortening fraction was comparable between DKO and WT mice, the DKO mice showed significant decrease in ejection fraction and increase in heart weight in response to TAC (Supplementary Fig. 2E–F).

### **DKO mice exhibit a switch to the fetal metabolic gene program in the heart**

The metabolic switch from fatty acid to glucose utilization in a stressed heart involves reactivation of the fetal gene program<sup>29</sup>. In DKO mice, we found that the major regulators of fatty acid metabolism, PPAR- $\gamma$  coactivator 1 $\alpha$  (*Pgc1 $\alpha$* ), and peroxisome proliferator-activated receptor alpha (*Ppara*), were significantly down regulated (Fig. 3A and Supplementary Fig. 3A). Consistent with this, expression of a panel of PGC1 $\alpha$  target genes, including mitochondrial *Cpt1* and 2, *Erra* and  $\gamma$ , *Tfam*, *Nrf-1* and 2 (Fig. 3B–C and Supplementary Fig. 3) were robustly reduced in DKO hearts compared to WT mice. Additionally, we observed suppression of *Pdk4*, a known inhibitor of glucose oxidation (Fig. 3D). These data shows that DKO hearts switch their substrate utilization from fat to glucose oxidation indicating a stress response.

To test whether the gene expression changes functionally reflect a metabolic switch in DKO hearts, we utilized *ex vivo* Langendorff heart perfusions. The DKO hearts demonstrated a decrease in oleate oxidation coupled with subsequent increase in glucose oxidation within 15 minutes of *ex vivo* analysis (Fig. 3E–F). We conclude that the decreased functional capacity in DKO hearts is linked to the metabolic alteration.

### **Individual loss of either FXR or SHP does not phenocopy the DKO hearts**

Recently, roles for FXR in myocardial injury<sup>30</sup> and SHP in cardiac hypertrophy<sup>31</sup> have been identified. Hence, we examined whether deletion of *Fxr* or *Shp* alone led to the altered metabolic gene expression profile in the DKO mice. To do this, we carefully analyzed the expression of fatty acid and glucose regulator genes in *FXRKO* and *SHPKO* hearts and



compared them to WT animals. Interestingly, the reduction in expression of metabolic genes including *Pgc1a*, *Ppara* and their downstream targets readily seen in the DKO hearts was not observed in the single knockouts. In fact, *Ppara*, *m-Cpt2* and *Pdk4* expression were upregulated in *FXRKO* mice (Supplementary Fig. 4A–E). In *SHPKO* hearts, there was a modest reduction in *m-Cpt1* and *Pdk4* expression (Supplementary Fig. 5A–E). The echocardiographic findings corroborated the gene expression data in that no contractile abnormality was observed in *FXRKO* mice or *SHPKO* mice, except for a slight reduction in heart rate in the latter compared to their WT littermates (Supplementary Fig. 4F; Supplementary Fig. 5F).

### **Bile acids are sufficient to mimic the heart dysfunction phenotype observed in DKO mice**

To determine the effect of acutely increased circulating bile acids on the heart, we injected WT mice with the bile acids, taurocholic acid (TCA), or lithocholic acid (LCA), or vehicle and performed pre- and post- injection sedated electrocardiography and echocardiography. Bile acid injections induced significant bradycardia in the naïve WT mice (Supplementary Fig. 6A). Acute exposure to bile acids did not change echocardiogram parameters, but modestly reduced the LV diameter (Supplementary Fig. 6B–C).

We next examined whether acute bile acid challenge alters the metabolic preference in the heart. Using the *ex vivo* Langendorff method, WT hearts were perfused with TCA. Compared to vehicle, TCA perfused hearts showed a rapid 50% decrease in the heart rate and cycle amplitude (myocardial force of contractility) (Supplementary Fig. 6D–E). This was accompanied by a dramatic 50% reduction in oleate oxidation within 15 minutes upon TCA perfusion (Supplementary Fig. 6F). These data demonstrates that excess bile acids directly cause metabolic and functional changes in the heart.

To identify the mechanisms by which bile acids cause metabolic alterations, we performed *in vitro* studies using both the primary mouse cardiomyocyte culture and the well-established cardiac HL-1 cell line<sup>20</sup>. We treated cardiomyocytes with the pathological concentration of chenodeoxycholic acid (CDCA) observed during liver diseases<sup>32</sup>. Remarkably, the high dose of CDCA dramatically suppressed FAO regulators such as *Pgc1a*, *m-Cpt1*, *Nrf-1*, *Nrf-2* and *Tfam* (Fig. 4A–D) in the primary cardiomyocytes, whereas bile acid treatment did not alter *m-Cpt2* (Fig. 4B) levels. Consistent with the data seen in DKO mice, *Pdk4*, a crucial inhibitor of glucose oxidation (Fig. 4E) was down regulated in the cardiomyocytes in response to CDCA.

Similarly, HL1 cardiac cells displayed modest but significant down regulation in these genes (Fig. 5) when challenged with high doses of CDCA. However, non-pathological dose of CDCA did not induce any alterations in the metabolic gene profiles (data not shown). It is important to point out that only pathological concentrations of bile acid was able to recapitulate both the functional and molecular changes in primary cardiomyocytes and HL-1 cells, as observed in the DKO mice hearts (Fig. 3–5).

### **Overexpression of *Pgc1a* rescues bile acid-induced metabolic alterations *in vitro***

Hearts from *Pgc1a* knockout mice demonstrate increased glucose oxidation and reduced FAO, highlighting that *Pgc1a* is a master regulator for cardiac metabolism<sup>33–35</sup>. Therefore

we examined if the metabolic effects of bile acids can be reversed by *Pgc1a* overexpression. We ectopically expressed *Pgc1a* in HL-1 cells, with increased levels maintained even upon CDCA incubations (Fig. 5A). CDCA mediated reductions in the levels of FAO genes *Ppara*, *m-Cpt1* as well as glucose oxidation gene *Pdk4* were de-repressed upon this overexpression (Fig. 5B–D).

### Decreasing serum bile acid levels completely rescued cardiac dysfunction in DKO mice

To determine if pathological bile acids were directly responsible for the observed cardiac defects, we treated DKO mice with Cholestyramine (CHR), a bile acid binding resin known to reduce circulating bile acid pool. As expected, the serum bile acid concentrations in the DKO mice robustly decreased to half the original DKO concentration upon treatment with CHR diet. This reduction is also reflected in the overall decrease in the bile acid composition (Fig. 6A).

M-mode ECHO analysis revealed that CHR feeding was sufficient to restore the functional cardiac parameters in the DKO mice including the heart rate and cardiac output to that of the control WT levels (Fig. 6B). Consistent with these data, left ventricular internal diameter (LVID) in both diastole and systole increased in the CHR fed DKO mice compared to its chow fed control (Fig. 6C). Furthermore, these functional changes were accompanied by up regulation of FAO genes *Pgc1a*, *m-Cpt1* and *m-Cpt2* (Fig. 6D–E). Taken together, these findings suggest that reducing circulating bile acid pools is sufficient to reverse the cardiac pathology associated with *Cholecardia*. The overall mechanism is summarized in Fig. 6F.

## DISCUSSION

A wide array of end stage liver diseases, including alcoholic cirrhosis<sup>36</sup>, chronic hepatitis B or C viral infections, and NAFLD<sup>37</sup> result in heart dysfunction<sup>1,4,38</sup>. However, the molecular mechanisms underlying this liver disease-dependent heart failure are not understood. Increased circulating levels of bile acids are observed in all these cases of liver dysfunction<sup>39</sup>, and are strongly associated with cardiomyopathy<sup>7,8,11,12,40</sup>. It has been previously shown that jaundice and/or cholestasis can impede  $\beta$ -adrenergic signaling and thus may lead to blunted cardiac contractility in these patients<sup>36</sup>. In this study we demonstrate that pathological levels of bile acids are sufficient to cause cardiac dysfunction and metabolic reprogramming (Fig. 4–6). We therefore propose the term *Cholecardia* to describe the syndrome of cardiac dysfunction in response to elevated bile acid levels.

The *Fxr;Shp* double knockout (DKO) mice are an excellent model for cholestatic liver disease, with elevated serum bile acids and enzymes ALT and AST (Supplementary Fig. 1). DKO mice exhibit cholestasis from an early age, and do not have acute pharmacologic and toxicologic confounders as observed in 3,5-diethoxycarbonyl-1,4-dihydrocollidine (DDC) and carbon tetrachloride model of end stage liver disease<sup>41,42</sup>.

One limitation of the DKO model is that it is a global, rather than a cardiomyocyte-specific *Fxr;Shp* deletion. We partially addressed this limitation by conducting *ex vivo* and *in vitro* experiments focusing on direct bile acid-myocardial interactions in WT cells with intact cardiomyocyte expression of FXR and SHP. Although there are some differences between



our model and cirrhotic patients (Supplementary Table 1), the DKO mice provide functional correlation to the clinical findings seen in human cirrhotic cardiomyopathy. Hearts of cirrhotic patients show hypertrophic left ventricle with diastolic dysfunction, prolonged QT interval and impaired response to exercise and catecholamine- induced stress. All these findings are phenocopied in the DKO mouse hearts, except for clinical tachycardia (Figs. 1 and 2, Supplementary Table 1). DKO mice instead exhibit bradycardia, which could be due to a direct inhibitory effect of bile acid on heart rate and rhythm as previously described<sup>11,43</sup>. In addition, DKO hearts show increased expression of cytoskeletal proteins along with activation of JNK and AKT (Fig.1 and Supplementary Fig.2), indicating molecular remodeling of DKO cardiomyocytes.

There is an intricate relationship between cardiac metabolism and function. It is well known that the perturbations in cardiac metabolism can precede contractile dysfunction, progressive left-ventricular remodeling and heart failure<sup>34,44</sup>. Therefore, we examined the metabolic gene expression profile in DKO hearts and found down regulation of a key coactivator and three nuclear receptors associated with FAO (*Pgc1a*, *Ppara*, *Erra* and *Errγ*). This reduction was reflected in decreased expression of target genes (*m-Cpt1 & 2*, *Nrf-1 & 2* and *Tfam*) and decreased preference for FAO in DKO hearts *ex vivo* (Fig. 3 & Supplementary Fig. 3)<sup>29</sup>. Moreover, the DKO heart exhibited suppression of *Pdk4*, a negative regulator of glucose oxidation, indicating an increase in glucose oxidation (Fig. 3). Together these results indicate a metabolic switch from fatty acid to glucose, which can function both as a “cause” and an “effect” of cardiac stress and can explain cardiac defects seen in the DKO mice.

Next, we tested if elevated circulating levels of bile acids, which are characteristic of the DKO mouse model as well as cirrhotic and non-cirrhotic liver diseases, are sufficient to induce myocardial defects<sup>14</sup>. It has been known that high levels of bile acids are toxic to the heart<sup>12,32,39</sup>; especially TCA has been directly linked to fetal arrhythmias, and poor cardiomyocyte contractility<sup>11,13,40,45</sup>. Moreover, bile acids are rapidly emerging as specialized signaling molecules<sup>46,47</sup> regulating metabolism and function of various tissues. They signal by both the nuclear receptor FXR and the G protein coupled receptor TGR5, both of which are expressed in the heart<sup>15</sup>. We found that bile acids rapidly and directly modulate heart function. WT hearts exposed to high concentrations of TCA showed a significant decrease in oleate oxidation within 15 min (Supplementary Fig. 6), suggesting that a metabolic mechanism accounts for the impact of bile acid excess on cardiac contractility.

We examined whether deletion of FXR or its downstream target SHP could account for the changes in myocyte function in DKO mice. FXR activation is known to promote vasodilation<sup>48,49</sup> whereas loss of FXR has been implicated in protecting against myocardial apoptosis<sup>30</sup>. We found that FXRKO mice maintain normal cardiac function and do not exhibit metabolic changes in the heart (Supplementary Fig. 4). Thus, loss of the bile acid sensor FXR is not the primary cause for the cardiac pathology seen in the DKO mice. On the contrary, deletion of SHP causes hypertrophy and bradycardia, along with a few changes in the metabolic gene expression pattern compared to DKO mice (Supplementary Fig. 5). Our data validates the recently described role for SHP in regulating cardiac growth<sup>31</sup>. It was shown that SHP is a novel anti-hypertrophic regulator that acts by interfering with GATA6

signaling in the heart<sup>31</sup>. Further studies in cardiomyocyte-specific *Fxr* and *Shp* single and double knockouts would be necessary to fully delineate the role of the FXR-SHP axis in the heart. It is possible that TGR5, the membrane G protein coupled bile acid receptor<sup>50</sup>, could mediate these responses. Further experiments will be needed to test the potential role of TGR5 in *Cholecardia*<sup>50</sup>.

Additionally, intra-peritoneal bile acid administration reproduced the decrease in heart rate (Supplementary Fig. 6) in WT mice, indicating a direct role for bile acids in rhythm disturbance that does not depend on the loss of FXR or SHP function. The reduction in rhythm seen in the DKO mice is in line with clinical findings in patients with obstructive jaundice called “icteric bradycardia”<sup>43</sup>.

At the cellular level, treating HL-1 cells or neonatal cardiomyocytes with CDCA, a primary bile acid in humans, mimicked the metabolic profile of DKO hearts, including a significant down regulation of *Pgc1a*, and *Pdk4* (Fig. 4 & 5) Reduction in *Pgc1a* levels is known to be sufficient to induce a number of cardiac defects. Moreover, *Pgc1a* knockout mice display a substrate switch from fatty acid to glucose<sup>33–35</sup>, which is consistent with our metabolic findings. Importantly, we have identified that these observed metabolic changes, upon bile acid overload, were rescued by restoration of *Pgc1a* expression (Fig. 5). These results suggest that *Pgc1a* down regulation, in response to pathologically elevated bile acid levels, is pivotal to the alteration in cardiac metabolic pathways.

Importantly, we discovered that reducing the burden of circulating bile acids with the bile acid binding resin cholestyramine (CHR) normalized the electrophysiological and functional competence of DKO hearts. These cardiac functional alterations were accompanied by increased expression of FAO genes (*Pgc1a*, *m-Cpt1* and *m-Cpt2*) along with inhibitor of glucose oxidation, *Pdk4* (Fig. 6).

Overall, our findings define a direct role for elevated bile acid levels in altering cardiac metabolism and function. Interrupting enterohepatic circulation of bile acids and promoting their excretion using CHR, or suppressing bile acid production via FXR activation could be novel potential therapeutic approaches to treat cirrhotic cardiomyopathy.

## Supplementary Material

Refer to Web version on PubMed Central for supplementary material.

## Acknowledgments

**Financial Support:** Startup funds from University of Illinois at Urbana-Champaign (SA), R03 HD080011 NICHHD (SA), P30 DK056338 (MD) and CPRIT RP120138 (DDM).

## Abbreviations

<i>Fxr</i>	Farnesoid X Receptor
<i>Shp</i>	Small Heterodimer Partner
<i>Pgc1a</i>	Proliferator-activated receptor- $\gamma$ coactivator 1 $\alpha$

<b>FAO</b>	fatty acid oxidation
<b>DKO</b>	<i>FXR and SHP</i> double knock out
<i>m-Cpt1/2</i>	mitochondrial-carnitine palmitoyl transferase-1/2
<i>Pdk4</i>	Pyruvate dehydrogenase kinase 4
<b>ALT</b>	Alanine Aminotransferase
<b>AST</b>	Aspartate Aminotransferase
<b>2DEcho</b>	Two-dimensional echocardiography
<b>%EF</b>	ejection fractions
<b>%FS</b>	shortening fractions
<b>AKT</b>	v-akt murine thymoma viral oncogene/Protein kinase B
<b>JNK</b>	c-Jun N-terminal Kinase
<i>β-MyHC</i>	β myosin heavy chain
<b>TAC</b>	Transverse Aortic Constriction
<b>LV</b>	Left ventricle
<i>Ppara</i>	Peroxisome proliferator-activated receptor α
<i>Err-α/γ</i>	Estrogen-related receptor alpha/gamma
<i>Nrf-1/2</i>	Nuclear respiratory factor-1/2
<i>Tfam</i>	Transcription factor A, mitochondrial
<b>CDCA</b>	Chenodeoxycholic acid
<b>TCA</b>	taurocholic acid
<b>LCA</b>	lithocholic acid
<b>and CHR</b>	Cholestyramine

## REFERENCES

1. Wiese S, Hove JD, Bendtsen F, Moller S. Cirrhotic cardiomyopathy: pathogenesis and clinical relevance. *Nat Rev Gastroenterol Hepatol.* 2014; 11:177–186. [PubMed: 24217347]
2. Alqahtani SA, Fouad TR, Lee SS. Cirrhotic cardiomyopathy. *Semin Liver Dis.* 2008; 28:59–69. [PubMed: 18293277]
3. Henriksen JH, Moller S. Cardiac and systemic haemodynamic complications of liver cirrhosis. *Scand Cardiovasc J.* 2009; 43:218–225. [PubMed: 19145534]
4. Zardi EM, et al. Cirrhotic cardiomyopathy. *J Am Coll Cardiol.* 2010; 56:539–549. [PubMed: 20688208]

5. Desai MS, et al. Cardiac structural and functional alterations in infants and children with biliary atresia, listed for liver transplantation. *Gastroenterology*. 2011; 141:1264–1272. 1272 e1261–1272 e1264. [PubMed: 21762660]
6. Torregrosa M, et al. Cardiac alterations in cirrhosis: reversibility after liver transplantation. *Journal of hepatology*. 2005; 42:68–74. [PubMed: 15629509]
7. Binah O, Rubinstein I, Bomzon A, Better OS. Effects of bile acids on ventricular muscle contraction and electrophysiological properties: studies in rat papillary muscle and isolated ventricular myocytes. *Naunyn Schmiedebergs Arch Pharmacol*. 1987; 335:160–165. [PubMed: 3561530]
8. Zavec JH, Battarbee HD. The role of lipophilic bile acids in the development of cirrhotic cardiomyopathy. *Cardiovasc Toxicol*. 2010; 10:117–129. [PubMed: 20414815]
9. Legg JW. On the bile, jaundice and biliary diseases. 1879
10. Joubert P. An in vivo investigation of the negative chronotropic effect of cholic acid in the rat. *Clin Exp Pharmacol Physiol*. 1978; 5:1–8. [PubMed: 639354]
11. Joubert P. Cholic acid and the heart: in vitro studies of the effect on heart rate and myocardial contractility in the rat. *Clin Exp Pharmacol Physiol*. 1978; 5:9–16. [PubMed: 639363]
12. Rainer PP, et al. Bile acids induce arrhythmias in human atrial myocardium—implications for altered serum bile acid composition in patients with atrial fibrillation. *Heart*. 2013; 99:1685–1692. [PubMed: 23894089]
13. Williamson C, et al. Bile acid signaling in fetal tissues: implications for intrahepatic cholestasis of pregnancy. *Digestive diseases*. 2011; 29:58–61. [PubMed: 21691106]
14. Anakk S, et al. Combined deletion of Fxr and Shp in mice induces Cyp17a1 and results in juvenile onset cholestasis. *J Clin Invest*. 2011; 121:86–95. [PubMed: 21123943]
15. Desai MS, et al. Hypertrophic cardiomyopathy and dysregulation of cardiac energetics in a mouse model of biliary fibrosis. *Hepatology*. 2010; 51:2097–2107. [PubMed: 20512997]
16. Rockman HA, et al. Segregation of atrial-specific and inducible expression of an atrial natriuretic factor transgene in an in vivo murine model of cardiac hypertrophy. *Proc Natl Acad Sci U S A*. 1991; 88:8277–8281. [PubMed: 1832775]
17. Young ME, et al. Impaired long-chain fatty acid oxidation and contractile dysfunction in the obese Zucker rat heart. *Diabetes*. 2002; 51:2587–2595. [PubMed: 12145175]
18. Young ME, Razeghi P, Cedars AM, Guthrie PH, Taegtmeier H. Intrinsic diurnal variations in cardiac metabolism and contractile function. *Circulation research*. 2001; 89:1199–1208. [PubMed: 11739286]
19. Ghose R, Zimmerman TL, Thevananther S, Karpen SJ. Endotoxin leads to rapid subcellular re-localization of hepatic RXRalpha: A novel mechanism for reduced hepatic gene expression in inflammation. *Nucl Recept*. 2004; 2:4. [PubMed: 15312234]
20. Claycomb WC, et al. HL-1 cells: a cardiac muscle cell line that contracts and retains phenotypic characteristics of the adult cardiomyocyte. *Proc Natl Acad Sci U S A*. 1998; 95:2979–2984. [PubMed: 9501201]
21. Heling A, et al. Increased expression of cytoskeletal, linkage, and extracellular proteins in failing human myocardium. *Circulation research*. 2000; 86:846–853. [PubMed: 10785506]
22. Ho D, et al. Heart Rate and Electrocardiography Monitoring in Mice. *Current protocols in mouse biology*. 2011; 1:123–139. [PubMed: 21743842]
23. Bernardi M, et al. Q-T interval prolongation in cirrhosis: prevalence, relationship with severity, and etiology of the disease and possible pathogenetic factors. *Hepatology*. 1998; 27:28–34. [PubMed: 9425913]
24. Arikian C, et al. Impact of liver transplantation on rate-corrected QT interval and myocardial function in children with chronic liver disease\*. *Pediatric transplantation*. 2009; 13:300–306. [PubMed: 18537904]
25. Depre C, et al. Unloaded heart in vivo replicates fetal gene expression of cardiac hypertrophy. *Nature medicine*. 1998; 4:1269–1275.
26. Heineke J, Molkentin JD. Regulation of cardiac hypertrophy by intracellular signalling pathways. *Nature reviews. Molecular cell biology*. 2006; 7:589–600. [PubMed: 16936699]

27. Mair J, Dienstl F, Puschendorf B. Cardiac troponin T in the diagnosis of myocardial injury. *Critical reviews in clinical laboratory sciences*. 1992; 29:31–57. [PubMed: 1388708]
28. Wong F, et al. The cardiac response to exercise in cirrhosis. *Gut*. 2001; 49:268–275. [PubMed: 11454805]
29. Taegtmeier H, Sen S, Vela D. Return to the fetal gene program: a suggested metabolic link to gene expression in the heart. *Ann N Y Acad Sci*. 2010; 1188:191–198. [PubMed: 20201903]
30. Pu J, et al. Cardiomyocyte-expressed farnesoid-X-receptor is a novel apoptosis mediator and contributes to myocardial ischaemia/reperfusion injury. *European heart journal*. 2013; 34:1834–1845. [PubMed: 22307460]
31. Nam YS, et al. Small heterodimer partner blocks cardiac hypertrophy by interfering with GATA6 signaling. *Circulation research*. 2014; 115:493–503. [PubMed: 25015078]
32. Barnes S, Gallo GA, Trash DB, Morris JS. Diagnostic value of serum bile acid estimations in liver disease. *J Clin Pathol*. 1975; 28:506–509. [PubMed: 1141454]
33. Arany Z, et al. Transcriptional coactivator PGC-1 alpha controls the energy state and contractile function of cardiac muscle. *Cell Metab*. 2005; 1:259–271. [PubMed: 16054070]
34. Lehman JJ, et al. The transcriptional coactivator PGC-1alpha is essential for maximal and efficient cardiac mitochondrial fatty acid oxidation and lipid homeostasis. *Am J Physiol Heart Circ Physiol*. 2008; 295:H185–H196. [PubMed: 18487436]
35. Lai L, et al. Transcriptional coactivators PGC-1alpha and PGC-1beta control overlapping programs required for perinatal maturation of the heart. *Genes & development*. 2008; 22:1948–1961. [PubMed: 18628400]
36. Ma Z, Zhang Y, Huet PM, Lee SS. Differential effects of jaundice and cirrhosis on beta-adrenoceptor signaling in three rat models of cirrhotic cardiomyopathy. *Journal of hepatology*. 1999; 30:485–491. [PubMed: 10190733]
37. Domanski JP, Park SJ, Harrison SA. Cardiovascular disease and nonalcoholic fatty liver disease: does histologic severity matter? *Journal of clinical gastroenterology*. 2012; 46:427–430. [PubMed: 22469639]
38. Zardi EM, et al. Cirrhotic cardiomyopathy in the pre- and post-liver transplantation phase. *J Cardiol*. 2015
39. Neale G, Lewis B, Weaver V, Panveliwalla D. Serum bile acids in liver disease. *Gut*. 1971; 12:145–152. [PubMed: 5548561]
40. Williamson C, et al. The bile acid taurocholate impairs rat cardiomyocyte function: a proposed mechanism for intra-uterine fetal death in obstetric cholestasis. *Clin Sci (Lond)*. 2001; 100:363–369. [PubMed: 11256973]
41. Brady AM, Lock EA. Inhibition of ferrochelatase and accumulation of porphyrins in mouse hepatocyte cultures exposed to porphyrinogenic chemicals. *Archives of toxicology*. 1992; 66:175–181. [PubMed: 1497480]
42. Recknagel RO, Glende EA Jr, Dolak JA, Waller RL. Mechanisms of carbon tetrachloride toxicity. *Pharmacology & therapeutics*. 1989; 43:139–154. [PubMed: 2675128]
43. Bashour TT, Antonini C Sr, Fisher J. Severe sinus node dysfunction in obstructive jaundice. *Annals of internal medicine*. 1985; 103:384–385. [PubMed: 3896086]
44. Russell LK, et al. Cardiac-specific induction of the transcriptional coactivator peroxisome proliferator-activated receptor gamma coactivator-1alpha promotes mitochondrial biogenesis and reversible cardiomyopathy in a developmental stage-dependent manner. *Circulation research*. 2004; 94:525–533. [PubMed: 14726475]
45. Gorelik J, et al. Taurocholate induces changes in rat cardiomyocyte contraction and calcium dynamics. *Clin Sci (Lond)*. 2002; 103:191–200. doi:10.1042/. [PubMed: 12149111]
46. Makishima M, et al. Identification of a nuclear receptor for bile acids. *Science*. 1999; 284:1362–1365. [PubMed: 10334992]
47. Sinal CJ, et al. Targeted disruption of the nuclear receptor FXR/BAR impairs bile acid and lipid homeostasis. *Cell*. 2000; 102:731–744. [PubMed: 11030617]
48. Li J, et al. FXR-mediated regulation of eNOS expression in vascular endothelial cells. *Cardiovascular research*. 2008; 77:169–177. [PubMed: 18006476]

49. He F, et al. Downregulation of endothelin-1 by farnesoid X receptor in vascular endothelial cells. *Circulation research*. 2006; 98:192–199. [PubMed: 16357303]
50. Kawamata Y, et al. A G protein-coupled receptor responsive to bile acids. *The Journal of biological chemistry*. 2003; 278:9435–9440. [PubMed: 12524422]

Author Manuscript

Author Manuscript

Author Manuscript

Author Manuscript



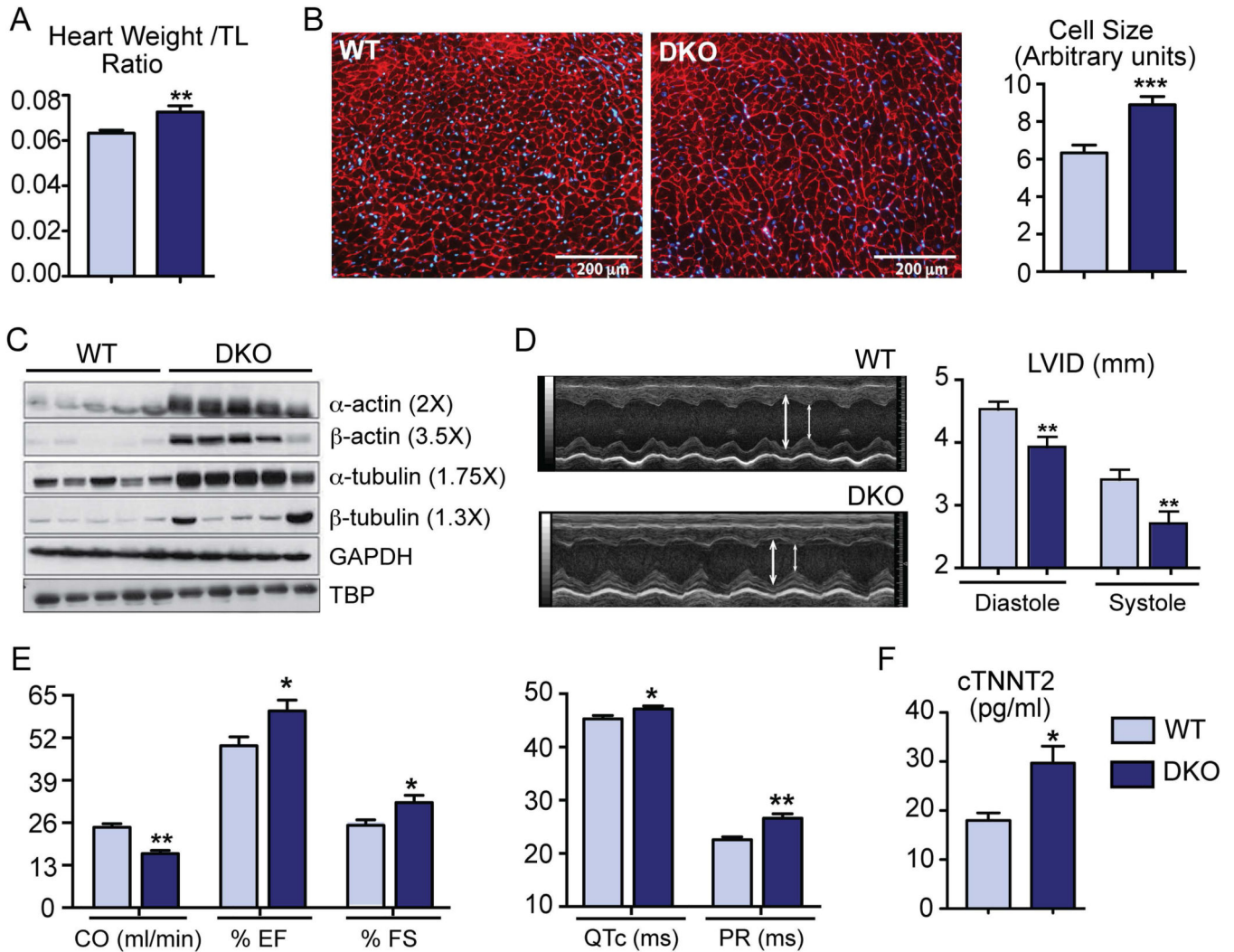


**Fig. 1. DKO mice show cardiac hypertrophy and abnormal cardiovascular parameters at baseline**

(A) Compared to WT, DKO mice exhibited increased heart weight to tibial length (TL) ratio. (B) DKO cardiomyocytes were bigger in size as quantified by WGA staining (n=2–3 mice/group; \*\*\*p<0.001). (C) Cardiac cytoskeletal proteins:  $\alpha$ / $\beta$ -actin and  $\alpha$ / $\beta$ -tubulin were induced in DKO hearts as seen by western blots. TBP was used as the loading control. (D) M-Mode ECHO images of the left ventricle displayed reduction in left ventricular internal diameter (LVID) in both diastole and systole in DKO mice. (E) Ejection fraction, shortening fraction, and QTc and PR interval were increased in DKO mice whereas cardiac output was reduced (F) ELISA for cardiac Troponin T showed induction in DKO mice. (n=6–12 mice / group; \*p<0.05; \*\*p<0.001 when compared to WT mice, Mean $\pm$  SEM)

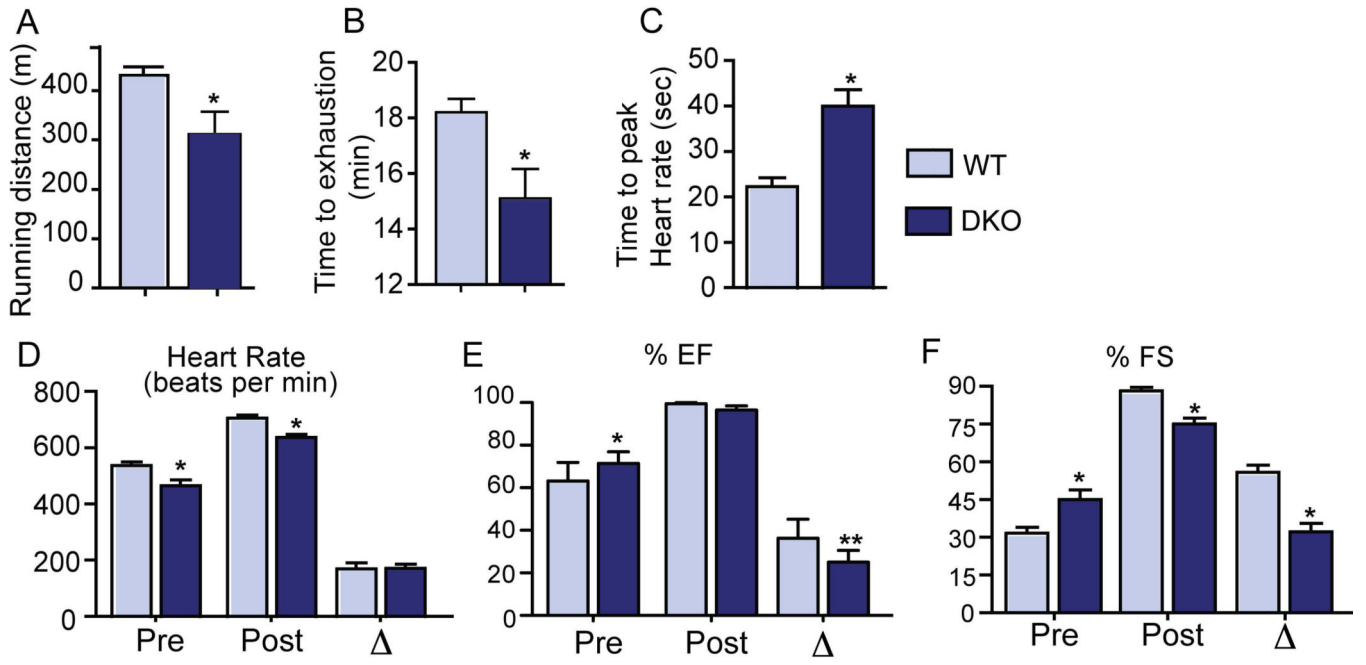


**Fig. 2. DKO mice demonstrate exercise intolerance and catecholamine insensitivity**  
WT mice were able to run more distance (meters) (A) and for a longer time (minutes) on the treadmill (B), compared to DKO mice. Upon isoprenaline challenge, DKO mice took longer to reach peak heart rate (C–D), and displayed lower changes in ejection fraction and shortening fraction (E–F). (n=5–6/group; \*p<0.05 when compared to WT animals; Mean ± SEM).

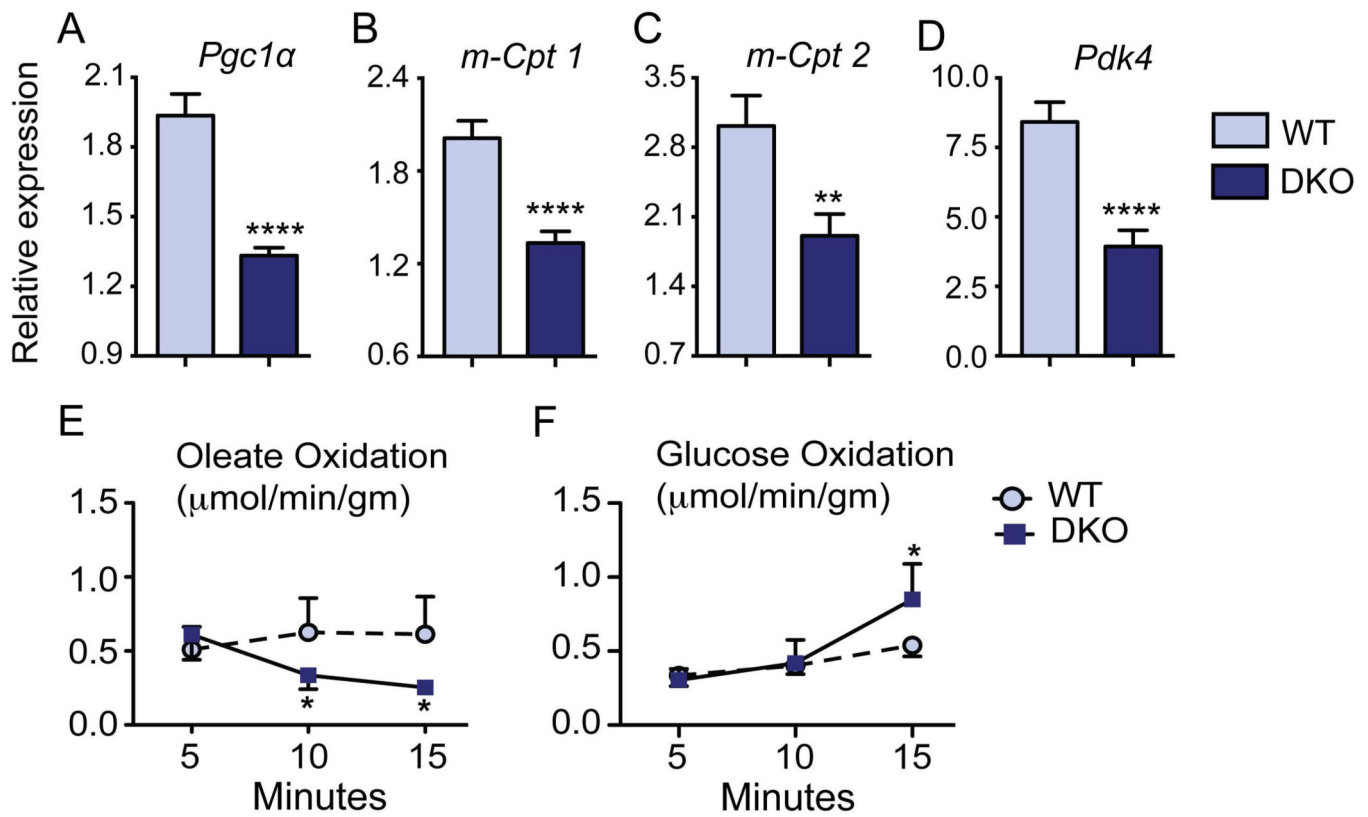


**Fig. 3. Metabolic switch occurs in DKO hearts**

Compared to WT, qRT-PCR analysis of DKO hearts revealed significant down-regulation of FAO genes *Pgc1α*, and *m-Cpt1/2* (A–C). Additionally, the regulator of glucose oxidation *Pdk4* was also altered in DKO hearts (D). All gene expression data were normalized to *36b4*. (E–F) Line diagram showed a switch from oleate to glucose oxidation in the DKO whole hearts mounted *ex vivo* on Langendorff apparatus. (n=5/group; \*p<0.05; \*\*\*p<0.0001 when compared to WT mice; Mean± SEM.)

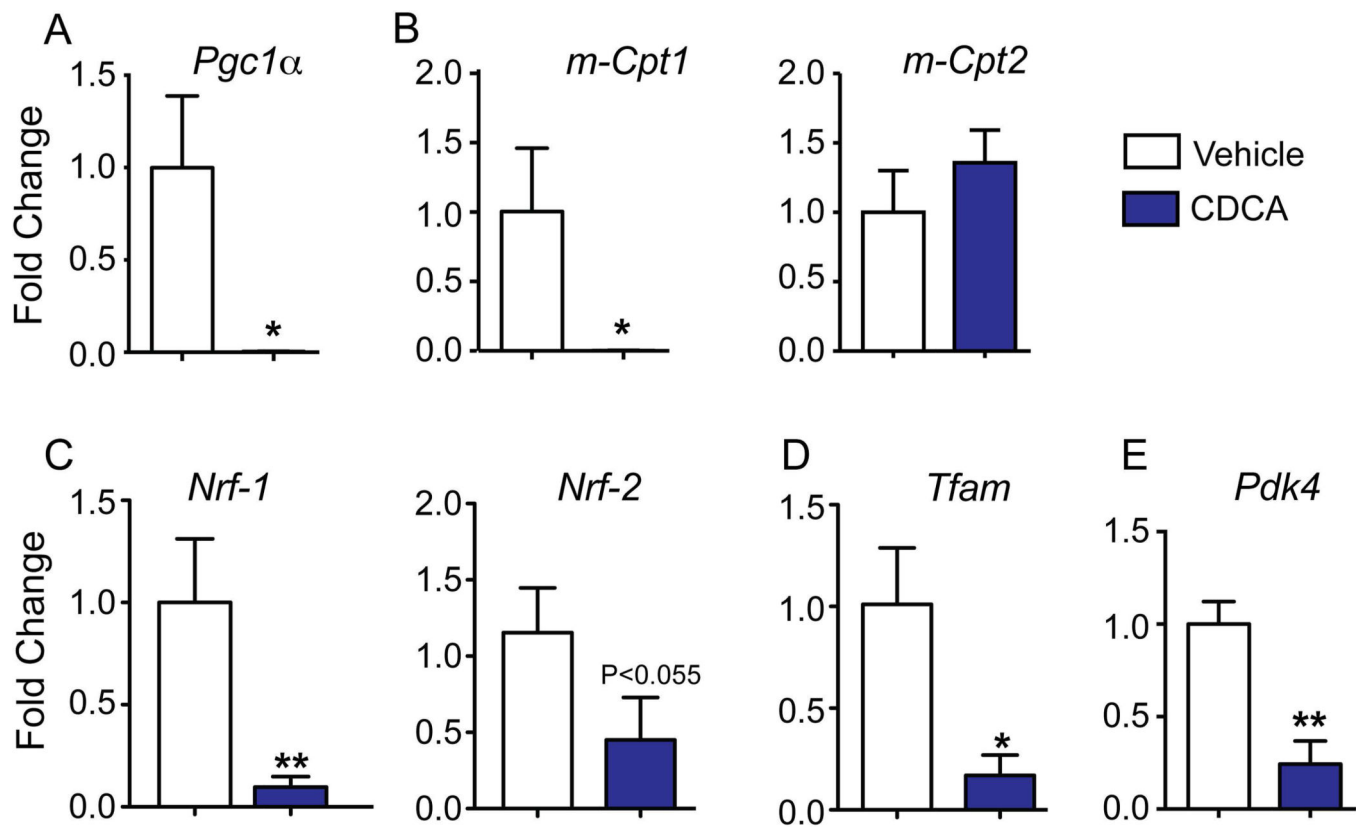


**Fig. 4. Bile acids are sufficient to suppress fatty acid oxidation genes in primary cardiomyocytes**  
 Neonatal cardiomyocytes, incubated with CDCA (100µM) for 4 hours, were evaluated for key genes regulating fatty acid and glucose oxidation. *18S* was used as the loading control. Values are depicted as fold change to Vehicle values (n=3 sets; \*p < 0.05; \*\*p < 0.001 compared to vehicle treated cardiomyocytes).

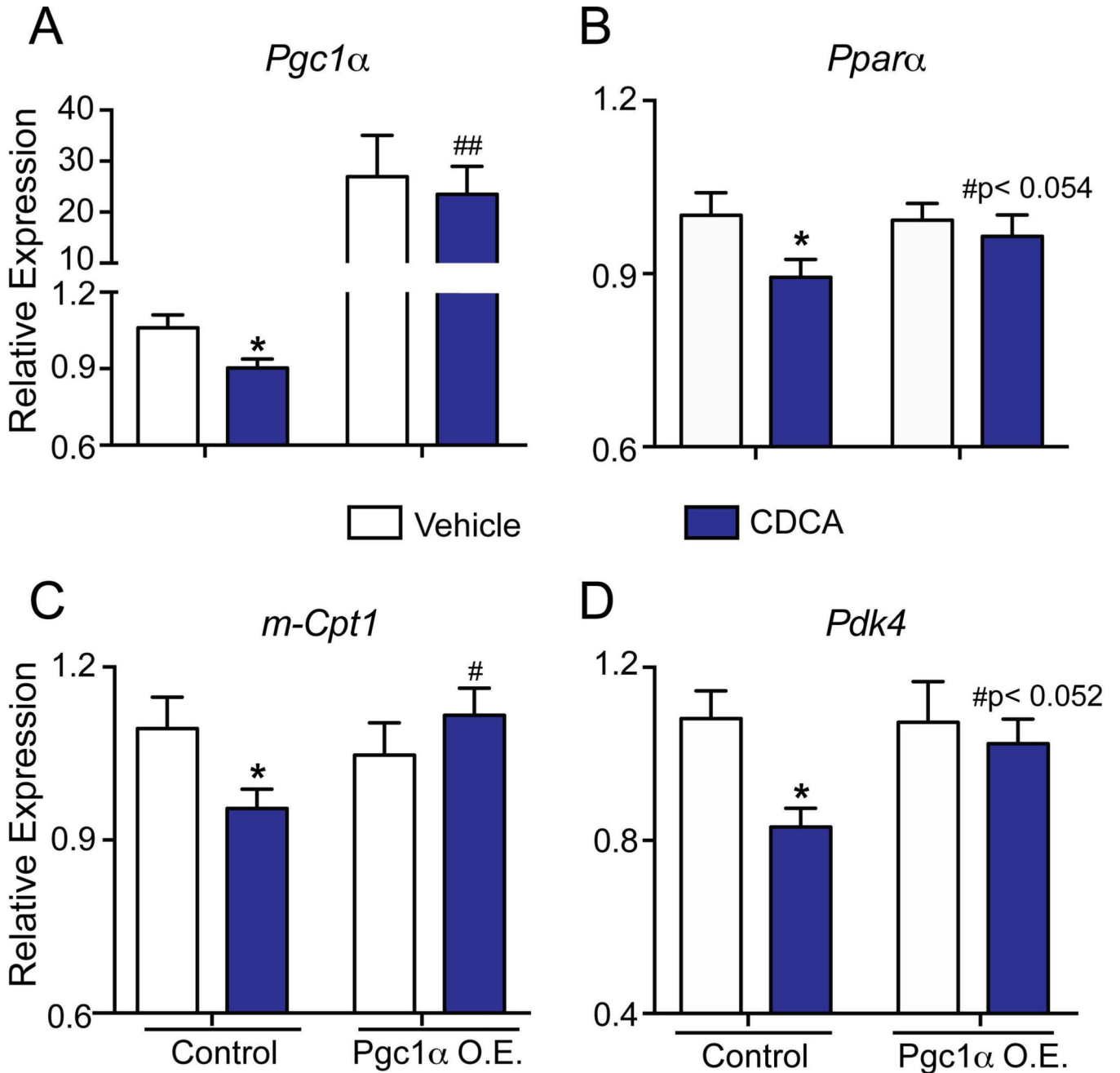


**Fig. 5. Overexpression of *Pgc1α* is sufficient to reverse bile acid-mediated alteration in metabolic genes**

*Pgc1α* was ectopically expressed in a cohort of HL-1 cells prior to CDCA treatments. CDCA mediated switch in metabolic genes *in vitro* was effectively rescued by *Pgc1α* overexpression. Gene expression was normalized to *36b4*. (n=4-6; \*p<0.05; compared to vehicle; #p < 0.05 compared to CDCA treated HL-1 cells; Mean±SEM).

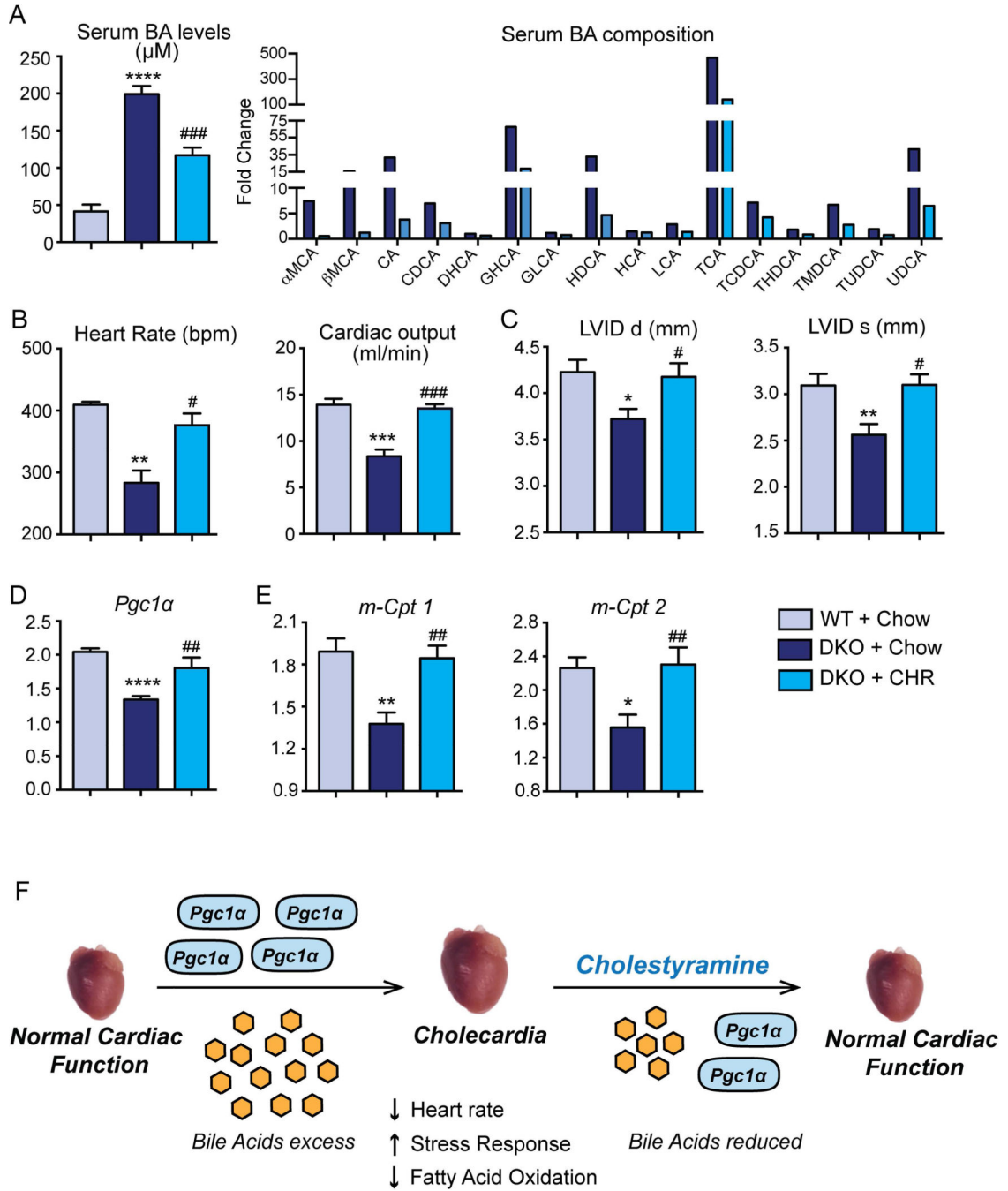


**Fig. 6. Reduction in circulating bile acid pools reverts the observed cardiomyopathy *in vivo*** (A) DKO mice fed Cholestyramine (CHR) exhibited 50% decrease in serum bile acid levels, compared to DKO mice on chow. Serum bile acid composition is shown as fold change to WT mice. (B) 2D ECHO analysis revealed normal heart rate and cardiac output in CHR-fed DKO mice. (C) Left ventricular internal diameter (LVID) in diastole and systole were restored to that of the WT level, when DKO mice were fed CHR. (D–E) The fatty acid regulator *Pgc1 $\alpha$*  and metabolic genes (*m-Cpt1/2*) were upregulated in DKO+CHR hearts compared to DKO+chow mice. The gene expression was normalized to *36b4*. (n=4–7 mice/



group; \*denotes  $p < 0.05$ , \*\* $p < 0.001$ , \*\*\* $p < 0.0001$  when compared to WT Chow; #denotes  $p < 0.05$ , ## $p < 0.001$ , ### $p < 0.0001$  when compared to the DKO Chow; Mean  $\pm$  SEM). (F) Proposed schematic indicating a mechanism by which bile acid overload can induce a metabolic switch in the heart, resulting in cardiac hypertrophy and dysfunction (*Cholecardia*).

Author Manuscript

Author Manuscript

Author Manuscript

Author Manuscript